On the dosimetry of megavoltage photon beams of very elongated fields

Author: Enric Sansalvador i Boadas
Facultat de Física, Universitat de Barcelona, Diagonal 645, 08028 Barcelona, Catalunya

Advisor: Dr. José M. Fernández-Varea

Abstract: In this TFG we have studied the Output Factors of 6 and 10 MV photon beams in small and elongated fields. We have compared the experimental data and the predictions of two treatment-planning systems from the Hospital de la Santa Creu i Sant Pau with Monte Carlo simulations done using the PENELOPE/penEasy code system. We have detected some discrepancies and tried to understand them.

I. INTRODUCTION

Radiotherapy is a therapeutic modality that, combined with surgery and chemotherapy, aims to achieve tumour control, i.e. the elimination of cancer cells, without damage to the surrounding healthy tissue. The radiation used in most radiotherapeutic treatments are megavoltage (MV) photon beams emitted by a linear accelerator (linac) which accelerates electrons and forces them to interact so as to produce bremsstrahlung. Since its introduction to nowadays, reducing the radiation exposure fields has been critial for one simple reason: the less healthy tissue that is irradiated, the less complications for the patient. However, the dosimetry of small fields presents specific problems such as the lack of lateral electronic equilibrium, the not flat lateral dose profiles or the fact that the perturbations introduced by detectors become less negligible.

Whereas in large fields the lateral dose is constant, in small fields the penumbra of the photon source gains importance which generates overestimated outputs from detectors and an increase of the uncertainties. Besides, as the effective region where detectors are useful to measure decreases, the physical dimensions of them could be not small enough to be appropriate.

A conventional parameter used to characterize photon beams is the so-called *Field Output Factor* (OF or Ω) which has another practical interest as well. Experimental OFs are one of the input data required to estimate absorbed-dose distributions with the clinical software utilised at the hospital. It is defined as the ratio of absorbed dose to water (D_{w}) in any clinical non-reference field (f_{clin}) to that in a reference field (f_{ref}) at a given depth [2]

$$\Omega^{f_{\mathrm{clin}},f_{\mathrm{ref}}}_{Q_{\mathrm{clin}},Q_{\mathrm{ref}}} = D^{f_{\mathrm{clin}}}_{\mathrm{w},Q_{\mathrm{clin}}} / D^{f_{\mathrm{ref}}}_{\mathrm{w},Q_{\mathrm{ref}}}, \tag{1}$$

here the subindex Q denotes the "quality index" of the incident radiation beam, which quantifies its penetration. For MV photon beams the quality index is given by the $\mathrm{TPR}_{20,10}$ ratio, the reference field is usually 10×10 cm^2 and absorbed dose is measured at a depth of 10 cm. In standard field, such as 8×8 cm^2 the absorbed dose D at a given point is proportional to the reading M of a detector placed at that point, so, OF can be obtained as the ratio of the detector readings. However, in small fields, this proportionality changes and several corrections must be applied to obtain valid experimental data. Here is where Monte Carlo simulations participate.

The aim of the present TFG has been to study the OF of 2×2, 2×12 and 2×30 cm^2 small, elongated fields for the TrueBeam0 linac from Varian for 6 MV and 10 MV photon beams. Simulation results obtained with the PENELOPE/penEasy code system have been compared to the experimental data from the Hospital de la Santa Creu i Sant Pau (HSCSP) and to the predictions of the AAA and Acuros treatment-planning systems.

II. MATERIALS AND METHODS

A. Monte Carlo simulations

PENELOPE is a program for the Monte Carlo simulation of the transport of electron, positron and photon in complex geometries made of arbitrary materials. It follows primary particles and secondary radiations through a given geometrical structure. The information needed to run a simulation is defined in four types of input files, namely geometry, material, energy spectrum and configuration files.

Firstly, the geometry file contains all information about where we would sent the radiation. It is based on canonical quadric surfaces; these are surfaces that fulfil $I_1x^2 + I_2y^2 + I_3z^2 + I_4z + I_5 = 0$ with $I_i = 0, \pm 1$. Once a surface is defined, it can be scaled, shifted and rotated in 3D space. Finally, a set of surfaces is used to set the bodies which would be filled up with a material of interest. Our geometry consists of a water phantom (body 3) whose dimensions are $64 \times 64 \times 53$ cm^3, the scoring volume (body 1) which is our "detector" formed by a thin parallelepiped (0.01 cm thick and with lateral dimensions that vary depending on the radiation field in order to optimize each simulation) and another parallelepiped which has allowed us to set the radiation field (body 2). Figure 1 displays an example of simulation geometry, where we have cut the water phantom in order to show the scoring volume.

Secondly, the material file contains all information about the physical properties, such as interaction cross sections or its mass density. We need as many materials

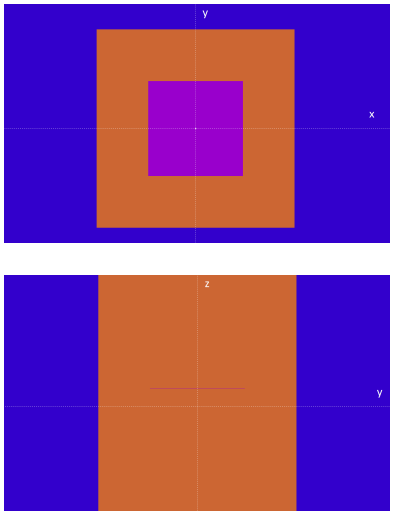

FIG. 1: xy (top) and yz (bottom) views of an example of simulation geometry. Body 1 is in pink, body 2 in orange and part of body 3 in blue.

files as materials are included in the geometry. In our case, we have just required one file for liquid water.

Thirdly, the spectrum file defines the energy distribution of the primary radiation. We have taken the 6 MV and 10 MV photon spectra with flattening filter from references [4, 5].

Finally, the configuration file includes the rest of important parameters such as the number of histories to be simulated, the coordinates of radiation source, or the absorption energies which from simulation no longer follows the particles (E_{abs}) depending on the material, as well as the output information we wish to obtain through the *tallies*. We have been simulating with 2×10^8 histories, $E_{\text{abs}} = 10$ keV for photons all over the geometry, $E_{\text{abs}} = 80$ keV for electrons and positrons in bodies 1 and 2 and $E_{\text{abs}} = 1$ MeV for electrons and positrons in body 3. Regarding the tallies, we have activated the *Tally Spatial Dose Distribution* which returns the absorbed dose distribution of a region of interest, the *Tally Energy Deposition* which scores the energy deposited by the radiation to all bodies defined in the geometry file, and the *Tally Fluence Track Lenght* which scores the differential fluence integrated over the detector volume.

B. $\text{TPR}_{20,10}$

The penetration of a MV photon beam is quantified by the quality index $\text{TPR}_{20,10}$, defined as the ratio of the absorbed dose at 20 cm depth to the absorbed dose at 10 cm depth for a distance between the detector and the source of 100 cm. It is a robust index because it is not affected by contamination electrons that may arrive to the surface of the patient. As HSCSP has provided the experimental $\text{TPR}_{20,10}$ values for their 6 and 10 MV beams, we can compare the $\text{TPR}_{20,10}$ obtained by simulating with the spectra from references [4, 5] and select, for the rest of simulations, the one that achieves the best agreement.

$\text{TPR}_{20,10}$ is defined in detail in section 6.3 of the TRS-398 protocol of the IAEA [2]. The conventional way to obtain this quality index is through method 1 and two simulations. However, reference [2] allows an alternative method, where $\text{TPR}_{20,10}$ is proposed to be calculated through method 2, which just need one simulation. These two different methodologies are described in the following subsection.

C. Calculation Methods

The next step is calculate the OFs. We have considered six methods to achieve it.

1. *Methods based on the definition of absorbed dose*

Absorbed dose is defined as the ratio of the mean energy imparted by ionising radiation, $\mathrm{d}\bar{\varepsilon}$, to a small volume of matter with mass $\mathrm{d}m$ [1]

$$D = \mathrm{d}\bar{\varepsilon}/\mathrm{d}m. \tag{2}$$

Method (1). The *Tally Energy Deposition* in penEasy delivers the energy imparted in the scoring volume and, knowing its volume and mass density, we can calculate the absorbed dose applying equation (2).

Method (2). Activating the *Tally Spatial Dose Distribution*. It calculates the absorbed dose to the region of interest with the discretization sought. Then, we fit an exponential function to the central-axis depth-dose curve in a depth interval between around 10 and 20 cm.

2. *Methods based on cavity theories*

Method (3). Related to the Bragg–Gray (BG) cavity theory [1]. ICRU defines cema (converted energy per unit mass) as the energy lost by charged particles, excluding secondary electrons generated by interactions, in electronic collisions in a mass of $\mathrm{d}m$ of a material. The Bragg–Gray cavity theory estimates absorbed dose to a cavity which is small compared to the range of electrons generated by a photon beam such as the ones used on radiotherapy and requires two conditions: (i) the cavity must not disturb the charged particle fluence in the absence of the cavity, (ii) the absorbed dose in the cavity is deposited entirely by the charged particles crossing it.

As OF is defined as the ratio of absorbed dose to water, our cavity should not distort the fluence and would not be difference between considering or not the cavity where we have simulated the fluence. Then, we can estimate the

absorbed dose to liquid water as

$$D_{\mathrm{w}}^{\mathrm{BG}} \approx \int_{\Delta}^{E_{\max}} \left[\Phi_E^{\mathrm{prim}}\right]_{\mathrm{w}} \left[S_{\mathrm{el}}(E)/\rho\right]_{\mathrm{w}} \mathrm{d}E + \left[\Phi_E^{\mathrm{prim}}(\Delta)\right]_{\mathrm{w}} \frac{\Delta}{\left[\rho r_{\mathrm{csda}}(\Delta)\right]_{\mathrm{w}}} \Delta, \tag{3}$$

where $\left[\Phi_E^{\mathrm{prim}}\right]_{\mathrm{w}}$ is the differential fluence (number of electrons per unit surface and unit energy) of *primary* electrons and $\left[S_{\mathrm{el}}(E)/\rho\right]_{\mathrm{w}}$ is the mass electronic stopping power which can be obtained by the relativistic Bethe formula [6]

$$\frac{S_{\mathrm{el}}(E)}{\rho} = \frac{C_0}{\beta^2}\frac{Z}{A}\left\{\ln\left(\frac{E^2}{I^2}\frac{\gamma+1}{2}\right) + F^{(-)}(\gamma) - \delta(\gamma)\right\}, \tag{4}$$

where $C_0 = 0.153\,537\ \mathrm{MeV\,cm^2\,g^{-1}}$, Z is the atomic number, A is the mass number, I is the mean excitation energy,

$$F^{(-)}(\gamma) = \gamma^{-2}\left[1 - (2\gamma-1)\ln 2 + \frac{1}{8}(\gamma-1)^2\right], \tag{5}$$

$\gamma = 1 + \frac{E}{m_e c^2}$, $\beta = \sqrt{1-\gamma^{-2}}$ and $\delta(\gamma)$ is the density-effect correction, parameterized in the form [7]

$$\delta(X) = \begin{cases} 10^{2(X-X_0)}\delta\left(X_0\right) & \text{if } X < X_0 \\ \mathcal{C} + 4.60517X + a\left(X_1 - X\right)^m & \text{if } X_0 < X < X_1 \\ \mathcal{C} + 4.60517X & \text{if } X_1 < X \end{cases} \tag{6}$$

with $X \equiv \log_{10}(\beta\gamma)$ and $\{X_0, X_1, a, m, \delta\left(X_0\right)\}$ are tabulated parameters.

$\left[r_{\mathrm{csda}}(E)\right]_{\mathrm{w}}$ is the csda range of electrons with energy E, and Δ is the cut-off energy of the electrons which go through the cavity. It is determined by solving the equation $\left[\rho r_{\mathrm{csda}}(\Delta)\right]_{\mathrm{w}} = \rho\ell$, where $\ell = 0.01$ cm is the smallest dimension of the cavity.

As the original tally from penEasy returns $\left[\Phi_E^{\mathrm{tot}}\right]_{\mathrm{w}}$ which is the differential fluence of all electrons, we had to modify the code and recompile the program to obtain $\left[\Phi_E^{\mathrm{prim}}\right]_{\mathrm{w}}$.

Method (4). Spencer and Attix (SA) proposed an extension of the BG theory that takes into account the finite range of secondary electrons that go through the cavity, assuming that below the cut-off energy Δ, charged particles can not cross the cavity, and above Δ, were assumed to escape entirely. Then

$$D_{\mathrm{w}}^{\mathrm{SA}} \approx \int_{\Delta}^{E_{\max}} \left[\Phi_E^{\mathrm{tot}}\right]_{\mathrm{w}} \left[L_{\Delta}(E)/\rho\right]_{\mathrm{w}} \mathrm{d}E + \left[\Phi_E^{\mathrm{tot}}(\Delta)\right]_{\mathrm{w}} \left[S_{\mathrm{el}}(\Delta)/\rho\right]_{\mathrm{w}} \Delta, \tag{7}$$

where $\left[\Phi_E^{\mathrm{tot}}\right]_{\mathrm{w}}$ is the differential fluence of *all* electrons, and $\left[L_{\Delta}(E)/\rho\right]_{\mathrm{w}}$ is the mass electronic stopping power restricted to energy losses smaller than Δ which can be calculated with an expression analogous to equation (4)

$$\frac{L_{\Delta}(E)}{\rho} = \frac{C_0}{\beta^2}\frac{Z}{A}\left\{\ln\left(\frac{E^2}{I^2}\frac{\gamma+1}{2}\right) + G^{(-)}(\gamma,\eta) - \delta(\gamma)\right\}, \tag{8}$$

with $\eta = \Delta/E$ and

$$G^{-}(\gamma,\eta) = \gamma^{-2} + \ln[4(1-\eta)\eta] + (1-\eta)^{-1} + \gamma^{-2}\left[(\gamma-1)^2\eta^2/2 + (2\gamma-1)\ln(1-\eta)\right]. \tag{9}$$

Notice that $L_{\infty}(E) \equiv S_{\mathrm{el}}(E)$.

Figure 2 illustrates the shape of $\left[\Phi_E^{\mathrm{prim}}\right]_{\mathrm{w}}$ and $\left[\Phi_E^{\mathrm{tot}}\right]_{\mathrm{w}}$, which are used to approximate the absorbed dose through the BG and SA cavity theories, respectively. The difference between total and primary electron differential fluences is obviously due to the secondary electrons generated by the interactions of photons in water.

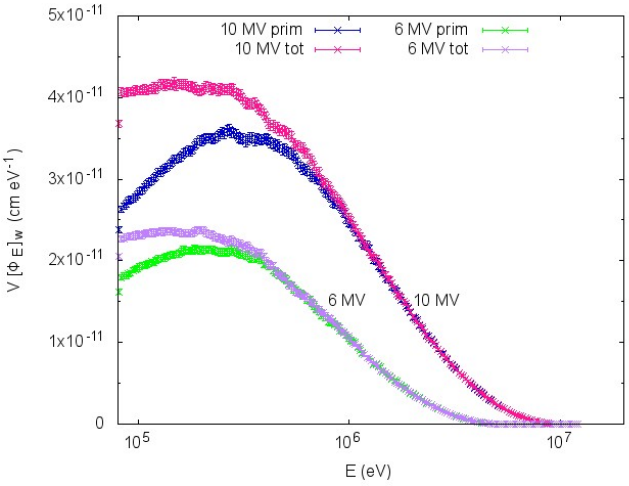

FIG. 2: Simulated differencial electron fluences, integrated over the detector volume placed at a 10 cm depth, generated by 6 MV and 10 MV beams for a 10×10 cm^2 field.

3. *Methods based on treatment-planning software*

Finally, we have obtained OFs from the treatment-planning systems used at the HSCSP. As Monte Carlo simulations are slow, medical physicists need fast algorithms for clinical use, such as AAA and Acuros. In contrast to PENELOPE, these methods use clinical experimental data such as dose profiles for many fields at various depths or OFs to make a model of the linac and calculate through it. AAA simulates the dose distribution superposing the attenuation of two photon beams (considering that the secondary photons generated by the multiple objects in the linac head are emitted from a hypothetical source) and an environment electron source (method 5). In turn, Acuros solves the linear Boltzmann transport equation (LBTE) which describes the macroscopic behaviour of the ionizing radiation in a deterministic and iterative way (method 6). More information can be found in references [9, 10].

III. RESULTS AND DISCUSSION

A. $TPR_{20,10}$

In order to choose appropriate photon energy spectra to use in the simulations of the OFs we had to calculate first the $TPR_{20,10}$ index as explained above. Throughout this project, all uncertainties quoted correspond to 2 SD.

Although the spectra published by Brualla and coworkers [5] are the most recent ones, from tables I and II we conclude that the spectra from reference [4] fit better to the experimental data. Hence, we have adopted the latter photon spectra for the subsequent calculation of OFs. At the same time, we conclude that the exponential adjustment, method 2, is a good alternative to calculate $TPR_{20,10}$ owing to its smaller uncertainty for a given simulation time.

TABLE I: $TPR_{20,10}$ ratios for the 6 MV photon beam.

	Ref. [4]	Ref. [5]
Method (1)	0.657(4)	0.647(4)
Method (2)	0.660(3)	0.650(3)
Experiment	0.665(6)	

TABLE II: $TPR_{20,10}$ ratios for the 10 MV photon beam.

	Ref. [4]	Ref. [5]
Method (1)	0.735(4)	0.723(4)
Method (2)	0.734(3)	0.724(3)
Experiment	0.736(7)	

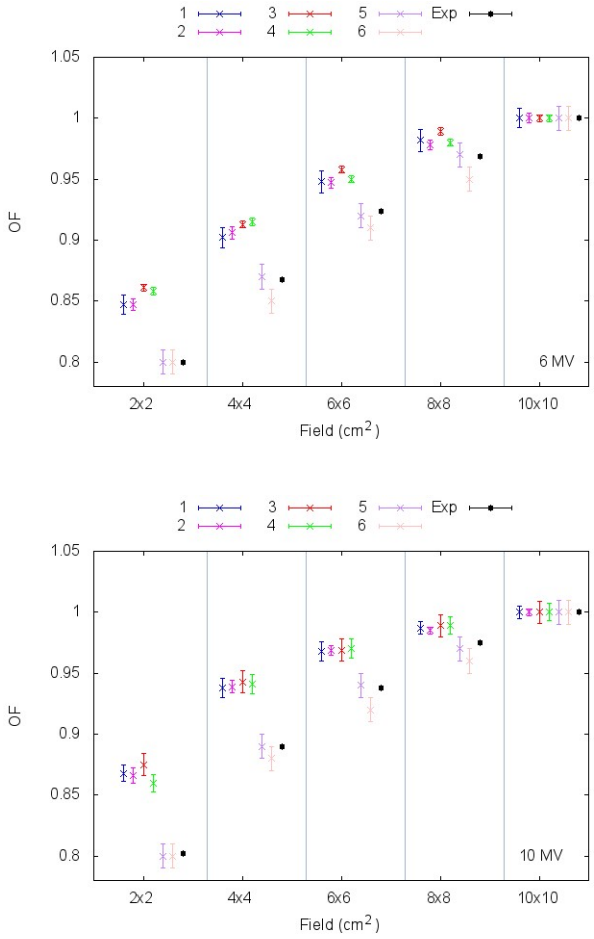

FIG. 3: OFs for 6 MV (top) and 10 MV (bottom) photon beams and various square fields.

B. Output Factors

Using the calculation methods described above, we have obtained the OFs shown in figures 3 and 4. We expected to obtain OFs similar to the experimental ones, but found large discrepancies. We will discuss below these results and the possible origin of the discrepancies.

On one hand, we can observe that both typology of methods from the Monte Carlo simulations data obtain concordant results. This fact express that through this project, we have checked the accuracy of the cavity theories, which means that calculating the absorbed dose from cavity integrals, equations (3) and (7), is equivalent to do it by means of its definition, equation (2). However, with the same number of histories simulated, the uncertainty obtained with methods 3 and 4 are significantly lower than for methodology 1, whose efficiency is poor, especially for small-field simulations. Method 2 makes a better use of the information generated by the simulation and slightly compensates this gap but, depending on the field and energy, it is not worth it compared to 3 or 4. Lastly, as method 4 is a more refined modification of the third one, it is expected to obtain better results. Generally, the main difference is related to the uncertainty, which is lower for the SA results.

On the other hand, we have found significant discrepancies between the Monte Carlo simulations and the experimental data and the results from the treatment-planning software. Reference [8] expresses the OF as the product of a factor related to the bremsstrahlung radiation generated in the linac head and another factor related to the secondary photons generated by the other objects from that linac head. The latter depends strongly on the volume of a virtual source that would generate these secondary photons. In typical radiation fields, primary photons find less artefacts to interact with and less secondary photons are produced. However, as in small fields the source is been occluded, the importance of secondary photons increase and the last factor related to OF gains ground. We have been working with a simplified geometry and primary photon spectra which do not include information about the energy distribution of these secondary photons. In addition, these spectrum assume that radiation is emitted isotropically, a too sim-

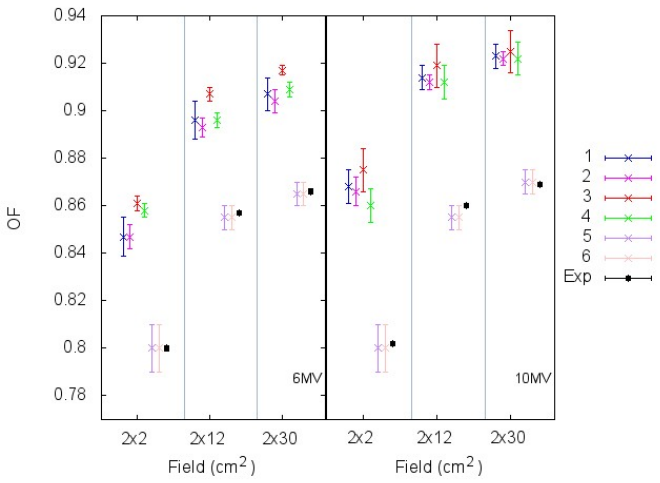

FIG. 4: OFs for 6 and 10 MV photon beams, elongated fields.

plified surmise for small fields. Figure 3 shows indeed that, as the field size grows, the discrepancy between simulated and experimental values is reduced. This behaviour agrees to the exposed argument.

One possible way to solve this problem would be to simulate the whole gantry of the linac. However, this solution has its own drawbacks. The first one is the difficulty to acquire the geometry of the linac. On our case, the accelerator model is the TrueBeam0 from Varian, who has a restrictive policy on sharing technical information about their models and the fact that creating the corresponding geometry file is not easy either. Finally, the simulations would be extremely time consuming and we would need a cluster of computers. Due to all these reasons, we have not been able to achieve better results.

Finally, concerning the treatment-planning systems, we observe that in spite of having a higher uncertainty, their results agree with the experimental ones. The reader needs to take into account that, while Monte Carlo simulations last around 1 day or more, AAA and Acuros deliver the results in around 1 or 2 minutes.

IV. CONCLUSIONS

Although the qualities of the MV photon beams simulated using spectra from reference [4] are similar to the experimental $TPR_{20,10}$ values, in small-field dosimetry this is not enough to guarantee that they will yield accurate OFs.

The calculations done with the cavity theories give similar results to those obtained from the definition of absorbed dose. Moreover, they achieve less uncertainty.

Although AAA and Acuros solve the problem of calculating the dose in a simplified way and obtain results with higher uncertainty, their results are acceptable, which is a proof they are consistent, and their simulation time is small enough to allow simulations in medical care system.

A complete study of the OFs needs more accurate photon energy spectra, geometry definition files and much more simulation time.

Acknowledgments

I am grateful to my advisor, Dr. José M. Fernández-Varea, for supervising and guiding me through this project. I would also like to thank Dr. Pablo Carrasco (HSCSP) for providing the experimental $TPR_{20,10}$ data and for his valuable help. Finally, I would like to thank my family and friends for their support and encouragement.

[1] Chavaudra, J., Nahum, A., Dance, D., Carlsson, G.A., Bielajew, A., Loverock, L. *Handbook of Radiotherapy Physics: Theory and Practice*, Edited by P. Mayles, A. Nahum, J.-C. Rosenwald, (Taylor & Francis, 2007) chapters 1, 2, 3, 4, 5, 6 and 11.

[2] International Atomic Energy Agency (IAEA). *Absorbed Dose Determination in External Beam Radiotherapy* (IAEA, Vienna, 2000) pp. 66–69.

[3] International Atomic Energy Agency (IAEA). *Dosimetry of Small Static Fields Used in External Beam Radiotherapy: An International Code of Practice for Reference and Relative Dose Determination*, (IAEA, Vienna, 2017)

[4] Sheikh-Bagheri, D., Rogers, D.W.O. Monte Carlo calculation of nine megavoltage photon beam spectra using the BEAM code. *Medical Physics* **29** (2002) 391–402

[5] Brualla, L., Rodriguez, M., Sempau, J., Andreo, P. PENELOPE/PRIMO-calculated photon and electron spectra from clinical accelerators. *Radiation Oncology* **14** (2019) 6 (10 pp)

[6] International Commission on Radiation Units and Measurements (ICRU). *Stopping Powers for Electrons and Positrons*, (ICRU, Bethesda, 1984). Sections 2, 7, 12 and tables 12.4 and 12.5.

[7] Sternheimer, R.M., Berger, M.J., Seltzer, S.M. Density effect for the ionization loss of charged particles in various substances. *Atomic Data and Nuclear Data Tables* **30** (1984) 261–271

[8] ESTRO, *Monitor Unit Calculation For High Energy Photon Beams – Practical Examples* (ESTRO, 2001)

[9] Van Esch, A., Tillikainen, L., Pyykkonen, J., Tenhunen, M., Helminen, H., Siljamäki, S., Alakuijala, J., Paiusco, M., Iori, M., Huyskens, D.P. Testing of the analytical anisotropic algorithm for photon dose calculation. *Medical Physics* **33** (2006) 4130–4148

[10] Vassiliev, O.N., Wareing, T.A., McGhee, J., Failla, G., Salehpour, M.R., Mourtada, F. Validation of a new grid-based Boltzmann equation solver for dose calculation in radiotherapy with photon beams. *Physics in Medicine and Biology* **55** (2010) 581–598